

STRUCTURAL QUALIFICATION OF SIR-C ANTENNA CORE STRUCTURE

Choon-Foo Shih* and Gordon Wang**

Jet Propulsion Laboratory
California Institute of Technology
Pasadena, California

ABSTRACT

A 2-bay SIR-C Antenna Core Structure (ACS) has been utilized to verify the strength of the SIR-C structural design. Five loading configurations were applied to assure that many SIR-C ACS members were loaded up to more than 1.25 times the predicted flight limit loads. The approach, test set-up, test procedures, testing results, and post-test evaluation are described in this paper. No structural failures were observed from the SIR-C static test. Testing results were also applied to update the SIR-C finite element model in order to provide a better test/analysis correlated model for the SIR-C modal survey and final coupled loads analysis. Analysis and component tests were also conducted to verify that the joints of the SIR-C structure were tested to the qualification levels without any failures.

INTRODUCTION

As the scientific use of radar data has become more sophisticated, the science potential of multifrequency and multipolarization data has become clear. NASA's Shuttle Imaging Radar-C (SIR-C) represents a significant step forward in the evolution of active radar remote sensing for the investigation of the Earth as an integrated system. SIR-C is the first spaceborne high-resolution imaging radar to provide multipolarization capability. It offers the first opportunity for simultaneous multifrequency radar imagery of the Earth from space as well as uses a high-efficiency dis-

tributed antenna array. In addition, the SIR-C missions will serve as a test-bed for several other innovations important in the development of the Synthetic Aperture Radar (SAR) to be flown on the Earth Observing System (EOS) polar platforms in the late 1990s.

The SIR-C missions are a cooperative venture featuring the NASA developed SIR-C and an X-SAR developed through joint collaboration with Dornier and Alenia Spazio Companies for the German space agency, Deutsche Agentur fuer Raumfahrtangelegenheiten (DARA), and the Italian space agency, Agenzia Spaziale Italiana (ASI). An international team of 49 principal investigators and three team associates - from universities, government agencies, and industry in 13 countries around the world, will be working in the broad range of disciplines that can benefit from the SAR data.

The SIR-C Antenna Mechanical System (AMS) has been designed and fabricated by NASA's Jet Propulsion Laboratory in Pasadena, California (Fig. 1). The SIR-C AMS is composed of three major structural components: the Antenna Core Structure (ACS), the Antenna Trunnion Structure (ATS), and the X-SAR Support Structure (XSS). The ACS provides a flat 3.5 meter by 12 meter mounting surface for the L-band and C-band radar array panels. The ATS ties the ACS to the Shuttle in a way that satisfies shuttle trunnion load-limitations and ACS mounting needs. The XSS provides a flat 0.5 meter by 12 meter mounting surface for the X-band radar array panels. The XSS is hinged to one edge of the ACS and controlled in tilt (rotation about x-axis) by a "tri-drive" actuator, and output crank, and a connecting strut.

* Technical Group Leader, Jet Propulsion Laboratory.

** Member of Technical Staff, Jet Propulsion Laboratory.

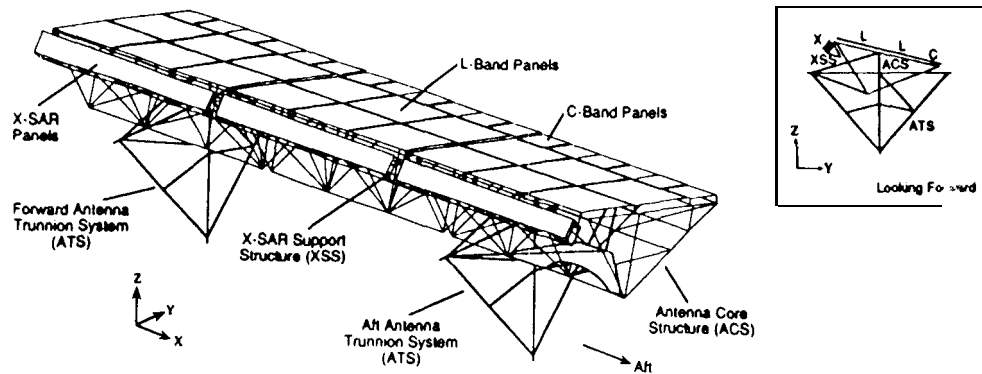


Fig. 1 SIR-C AMS Structural Elements

As specified in the "SIR-C Antenna Mechanical System (AMS) Structural Verification Plan," (Ref.1), static test of a 2-bay ACS module was required to verify the strength of a representative section of the SIR-C AMS structure. This 2-bay ACS module (Fig.2) has been selected for the SIR-C static test because it contains the most highly loaded ACS members, joints, and the x-axis shear panel. The objective of this static test is to demonstrate the structural integrity of the SIR-C AMS. Particularly, strength of low margin members and representative joints were verified through the static test. In addition, results of static test were applied to verify the stiffness and loads distribution predicted by the "finite element model" which was applied in the SIR-C coupled loads analysis. Details of the SIR-C static test setup, approach, and test procedures are described in Ref.2. The testing results and test/analysis correlation are thoroughly discussed in Ref.3.

TEST SETUP

Ground Support Interfaces

The 2-bay ACS module were tied down to the floor through the keel member and two 3 x 3 longerons at the corners of the test article. The 3 x 3 Al. longeron was held by 4 one-inch steel angles with two 3/4 inches steel bolts in double shear. Each angle was bolted down to a two-inches thick steel plate with two 3/4 inches

steel bolts. The base steel plate was then bolted to the ground with at least three 1 1/8 inches anchor steel bolts. Similar steel angles were used in the keel interface. All the steel bolts, angles, and base plates were designed to have a minimum safety factor of 3.5 on yield.

Load Linkage and Maintainer

Five hydraulic rams were used in the test to apply loads. Two rams (each has 50 Kips loading capability) with load cells were used to apply loads to the shear panel (attached to the keel member) against the ground. Another two 20-Kips rams and one 5-kips ram were applied to connect the top of C-band longeron and L-band longeron to the test tower interfaces. The linkages including the ram and load cell were proof loaded to 1.5 times the test apply loads prior to the actual test. The end attachments (brackets/lug) are designed to have a minimum safety factor of 3.5 on yield.

The Edison Load Maintainer was used in SIR-C static test to control the loading processes. Five out of the ten available channels were used for the static test. All the hydraulic lines connected to the hydraulic rams from the load maintainer were bled prior to the test load application. Each weight basket was individually calibrated for every specific load application.

Instrumentation

Phase I load application for a particular test configuration was up to 60% VLL (validation limited load) in three 20% VLL increments. The validation limit load is defined to be 1.25 times the limit load. Then the load was reduced to zero and test was halted while the measured data were evaluated. Prior to the phase II loading procedure, the test limits on highly loaded members were reset for the bar chart display based on the measurements from the Phase I tests.

In the Phase II load application, loads were applied to 60% VLL first and then be maintained at the 60% while all significant testing loads and predictions were verified to be within 5% of the expected values. Once this was accomplished, the test then proceeded to 100% VLL. Data were taken at every 10% increments (70%, 80%, 90%, and 100% of VLL) during this phase II loading procedure

Limit Control

Two levels of limit control were used in the Data Acquisition System (DAS) to provide an automatic test shutdown feature. Limit control levels were established after the phase I loading and introduced into the DAS for the phase II test. The first limit control was set at 104% of the expected VLL with an audio alarm. The second limit control was set at 108% of the expected VLL with a hydraulic dump feature. During the phase II test, most of the critical members had both limit controls. However, the hydraulic rams had only the level II limit control and they were verified with the correct load maintainer balance arm weights and pressure relief valve settings prior to the actual test load applications. In addition, a manually operated switch was installed in order to trigger a hydraulic dump in case of any emergencies.

Loading Configurations

Five loading configurations were selected to apply the external loads in the SIR-C static test. The first loading configuration (Figure 3.1) is the x-axis loading. Two jacks push the shear panel in the x-axis with 28 Kips from each jack. Analytical results indicate that 3 longerons and one batten will be loaded up to more than the validation limit loads. The second loading configuration is a y-

axis bending configuration (Figure 3.2). The test article were pulled in the same direction (z-axis) at the top of the corner longerons. One 3-D batten and 2 2-D battens were loaded up to more than the expected VLL. The applied loads of this loading configuration are 2330 (lbs) from each jack. The third loading configuration is a z-axis bending configuration (Figure 3.3). The applied load is from the jack (11.4 Kips) located at the top of the L-Band longeron in the lateral direction (y-axis). This loading configuration

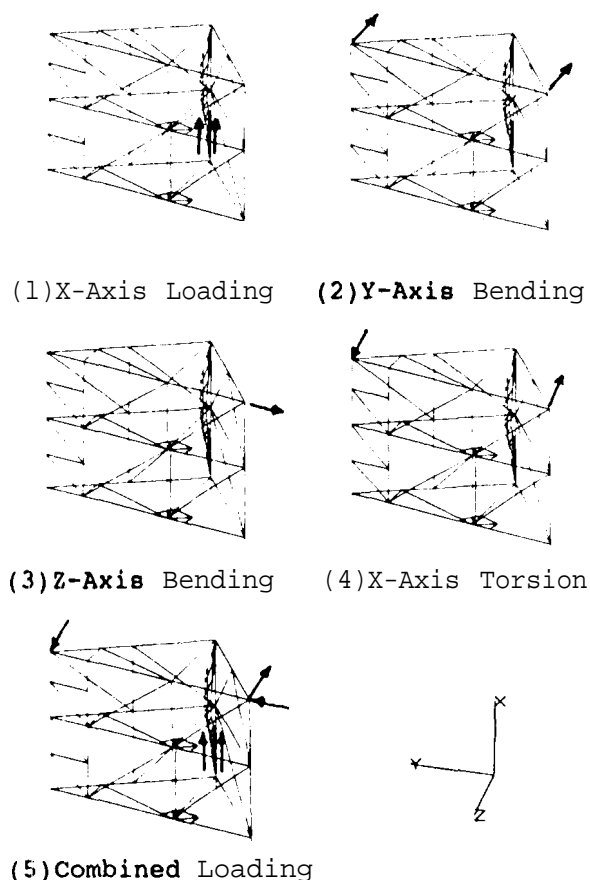


Fig. 3 Loading Configurations of SIR-C Static Test

develops higher loads mainly in the 2-D members. Analytical prediction indicates that 8 2-D members will be loaded up to more than the expected VLL. The fourth loading configuration is a x-axis torsion configuration (Figure 3.4). This configuration is similar to the second loading configuration except that loads ap-

plied to both **jacks** are in the **opposite directions**. Three members are expected to be loaded up to more than the **VLL**. The fifth loading configuration is a combined loading (Figure 3.5). It consists the **x-axis** loads from two big jacks (32 **Kips** each), the uneven **z-axis** loads on the corner **longerons** (2200 **lbs** and 2450 **lbs**), and the **y-axis** lateral load on the **L-band longeron top** (600 **lbs**). More than 7 members are expected to be loaded up to more than the **VLL** and several other members are expected to be loaded up to very close to the **VLL**.

RESULTS AND DISCUSSION

Thorough examination on the test article, particularly **joints**, was conducted after the completion of the final test (No. 5). No structural failures were observed. However, permanent sets of rivets in a number of joints were noted from the visual inspections. Two types of rivet elongation were observed as shown in Figure 4. The **first type** is the rivet head separation from the joint plate (up to more than 0.01") and the second type is the gapping between joint plates (up to more than 0.02").

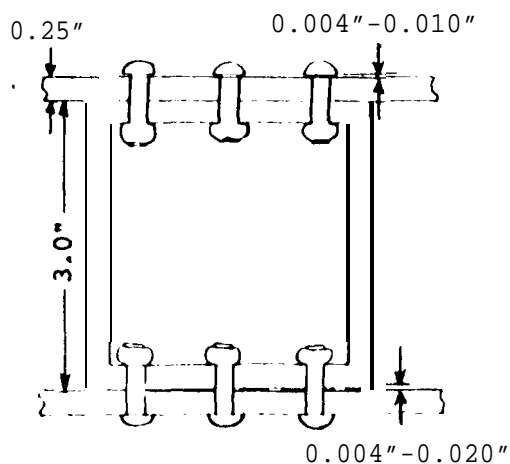


Fig 4 Types of Rivet Yield

No audible "pop" was heard during tests No. 1 through No. 4. However, two "pop" sounds were heard during test No. 5. The **first "pop"** occurred during the loading procedure from 60% **VLL** to 70% **VLL**. The second "pop" was heard when the test article was being loaded from 90% **VLL** to 100% **VLL**. The suspected "pop" **rivets** were identified. Although the rivet elongation

of these two rivets are large (0.01"), the shear carrying capability of these two **rivets** are considered to be intact (rivets were not broken and could not be pulled out by mechanical means). Detail joint analyses and joint tests are addressed in later Section.

Loads distribution of the test article was verified by using strain gages. 36 1/4-bridge strain gages were used to measure the **axial forces** of selected members and 12 1/2-bridge strain gages were applied for the moment measurements. Results of loads distribution from the 5 loading configurations are thoroughly summarized in Ref.3. The comparison between the predictions and the measurements indicates that very good correlations are observed for the axial forces. However, the moment comparisons suggest that the end conditions of some members required to be modified. Detail model modifications are discussed in next Section.

The stiffness comparisons are conducted by using the measured deflections from the **LVDTs**. A typical load vs. deflection plot from the first loading configuration is shown in Figure 5. It includes both the Phase I and Phase II results for the grid point No. 3032-z as shown in Figure 2. Two curves from the phase II tests are shown in Figure 5 since the first phase II was dumped at 99% **VLL** due to the improper limit control. Testing results indicate that the test article is nonlinear, particularly at the higher load levels. It is also noted that permanent deflections are measured after the unloading. It is interesting to note that the structure behaves much more linearly at the second time of loading. For instance, the phase I load/deflection curve of the grid No. 3032 is very nonlinear, but the first phase II load/deflection curve is very linear up to the 60% of the **VLL**. Nonlinearity of the first phase II test starts at 70% **VLL**. However, the second phase II load/deflection curve is fairly linear because the first phase II test was loaded up to 99% **VLL**. Similar results are observed from loading configuration 2 to 5. The discrepancy becomes more significant (percentage wise) as the tests are proceeded. Large displacements (more than 0.33") were measured in the test of loading configuration 5.

This is believed due to the rivet yield from the previous loading configuration. However, the load distribution measurements of this case still correlated well with the predictions.

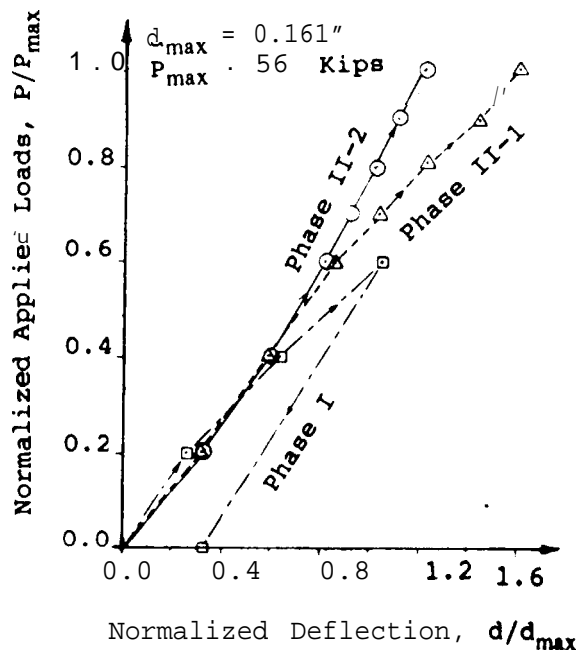


Fig. 5 Load/Deflection Curves

MODEL CORRELATIONS

As mentioned above, the measured moments of selected members do not correlate well with those predicted from the finite element model. Particularly, moment measurements of members No. 3543 and No. 3006 had the biggest discrepancy. The small moments measured from member No. 3543 (3-D diagonal) in all 5 loading configurations suggest that the end conditions of the 3-D joints should be pin type joints in both bending axes. The large discrepancy of the member No. 3006 also suggests that the pin flag used in the finite element model is not adequate for the 2-D vertical cross members. Proper end condition for these members should be rigidly connected. Table 1 shows that the moment correlation was improved significantly when these end conditions were modified in the finite element model. Results also indicate that this modified finite element model provides very good predictions on the axial forces.

Table 1 Loads Correlations from Selected Members

Element No.	Test Result	Predictions		
		(A)	(B)	(C)
3003*	7076	7011	7152	7197
3002*	6400	6438	6310	6404
3001*	5912	6051	5786	5938
3000*	5977	6556	6115	6269
3020*	9525	9857	9895	9788
3535*	33551	29594	29547	29635
3538*	-11678	-12822	-12853	-12848
3556*	15576	13646	13602	13487
3528*	6011	6797	6271	6468
3527*	6191	6852	6533	6740
3526*	7791	8297	8189	8157
3525*	14698	15971	15859	15903
3543*	-8538	-9754	-9120	-9381
3541*	-5190	-5640	-5331	-5667
3547*	16056	16457	16400	16668
3550*	11490	12507	12419	12506
3549*	-11628	-12581	-12498	-12536
3526**	609	258	332	1064
3543**	6	876	748	0
3006**	2731	351	1961	2027

* Strain gages for axial forces (lbs)

** Strain gages for bending moments (lb-in)

(A): Original finite element model

(B): Modified model with rigidly connected ends for 2-D vertical members

(C): Model (B) with pinned ends for all 3-D members

In order to obtain a better stiffness correlation for the finite element model used in the modal test correlation, the stiffness of the 2-D members and the 3-D members are reduced to account for the rivet joint flexibility by reducing their modulus of elasticity. Based on the measured displacement obtained from the 20% loading of the first loading configuration, the stiffness of the 3-D members should be reduced to 81%. Similarly, based on the results from the loading configuration 3, the stiffness of the 2-D members should be reduced to 67%. Table 2 indicates that reducing the stiffness of the 2-D members only affects the deflections measured in loading configuration 3. It is also noted that the stiffness of 3-D members do not affect the deflections developed in loading configuration 3. Table 2 shows that better correlations are observed if these stiffness reductions are incorporated in the finite element model. It is also noted that the stiffness modification does not affect the axial force correlation. However, the moment correlation is slightly influenced. In addition,

due to the compact **joints** of the C-band **longerons** and battens, the moments of inertia of the C-band **longerons** and battens are **increased** 40% to reflect the contribution of the joint plates. It is noted that this modification only **slightly affects** the **loads** distribution and deflections.

Table 2 Stiffness Correlations of SIR-C Static Test (in.)

	LVDTS	3032-z	3003-Y	3003-z
	Test	<u>0.211</u>	0.011	-0.190
	Model(A)	0.161	-0.005	-0.187
Test	Model(C)	0.163	-0.005	-0.183
Config.	Model(D)	0.166	-0.006	-0.197
1	Model(E)	0.204	-0.006	-0.238
	Model(F)	0.204	-0.006	-0.237
	Test	-0.083	0.018	<u>0.174</u>
	Model(A)	-0.044	0.017	0.121
Test	Model(C)	-0.044	0.017	0.120
Config.	Model(D)	-0.044	0.020	0.131
2	Model(E)	-0.053	0.024	0.156
	Model(F)	-0.053	0.024	0.156
	Test	0.084	<u>0.187</u>	<u>0.171</u>
	Model(A)	0.069	0.083	0.087
Test	Model(C)	0.069	0.083	0.086
Config.	Model(D)	0.086	0.103	0.107
3	Model(E)	0.102	0.122	0.128
	Model(F)	0.102	0.122	0.128
	Test	0.103	0.056	<u>0.193</u>
	Model(A)	0.062	0.040	0.140
Test	Model(C)	0.062	0.040	0.139
Config.	Model(D)	0.069	0.050	0.156
4	Model(E)	0.083	0.060	0.186
	Model(F)	0.083	0.060	0.185

Models (A) and (C) are described in Table 1.

Model (D): Model (C) with 2-D members' **stiffness** reduced to 80%.

Model (E): Model (C) with 2-D members' **stiffness** reduced to 67% and 3-D members' **stiffness** reduced to 81%.

Model (F): Model (E) with 40% increased moments of inertia for C-Band **longerons** and battens.

All these modification have been incorporated in both the "static test finite element model" and the "flight finite element model," which are used to verify the static test **results** and modal test **correlations**(Ref.4).

JOINT EVALUATION

Large deflections and permanent sets observed in the SIR-C static test are considered to be due to yielding of rivet joints. Therefore, detail investigations of the joints subjected to the testing loads were conducted

in order to obtain a better understanding of the joint loads during the tests and the individual rivet loads of **these** joints.

The members of the SIR-C test article can be categorized to be 8 kinds of member/joint connections and the keel member, as shown in Table 3. The maximum flight limit loads and the maximum testing loads from the 5 loading configurations are summarized in Table 3. It indicates that the joints, which connect the L-band

Table 3 Maximum Joint Loads of SIR-C Static Test(lbs)

Member/ Joints	Max imum <u>Limit Load</u>	Max imum <u>Test Load</u>
Longeron,L	10804	9525 (1)
Longeron,C	6540	7311 (3)
Batten,L	2787	5220 (3)
Batten,C	2223	2780 (2)
Diagonal,L	5945	7345 (3)
Diagonal,C	3017	2878 (3)
3-D Chord	16578	16026 (5)
3-D Diagonal	18991	20962 (5)
Keel Member	32992	37342 (5)

Numbers in () are the loading **configuration** numbers

batten, L-band diagonal, and the C-band batten were tested to equal to or more than the maximum validation limit loads (1.25 times flight limit loads). It is **also** noted that other types of joints are tested to the load levels which are close to the maximum flight limit loads.

In order to evaluate the rivet loads of the joints from the SIR-C static test, the modified finite element model was applied to derive the forces and moments of the investigated joints. Four kinds of joints are evaluated in **this** study. Maximum loads generated from all 5 **test** configurations were applied in **these** joints. Finite element models were established to investigate the rivet loads of various rivet patterns of these joints. Results of maximum rivet loads of these joints are summarized in Table 4. Results indicate that the maximum rivet loads **generated** from the static test are lower than the design ultimate rivet load (2215 **lbs** in single shear) and very close to 1.25 times the design limit load of the rivets (1064 **lbs**).

Table 4 Maximum Rivet Loads Established in SIR-C Static Test (lbs)

Joint Type	Element No.	Max. Rivet Load
3-D Diagonal	3547	2760*
C-Band Longerons	3003	1057
L-band Longerons	3020	1061
2-D Diagonal	3601	568(1412**)

* Double Shear

**Including warping effect

It should **also** be pointed out that the members used in the SIR-C static test article are the discarded **spares** from the flight hardware. Two of the **members**, a 2-D diagonal member and a 2-D L-band batten, were identified to have more than 1/4" warps. **Stress analysis** indicates that the maximum rivet loads of **these two joints** are 1408 (lbs) and 1412 (lbs), respectively (based on the assumption that the warp is 1/4"). These rivet loads are also lower than the design ultimate load and higher than 1.25 times the **design** limit load.

JOINT TEST

Two types of joint **tests** were conducted to validate the strength of rivet joints **used** in the SIR-C structure application. The first **test** is to validate the rivet's ultimate strength by using the INSTRON machine to pull single shear samples. **Testing results** from a number of **tests** indicate that the ultimate strength of these rivets is 2550 lbs, which is higher than the design ultimate rivet load provided from the manufacturer (2215 lbs). Typical results of single shear tests indicated that permanent sets were developed after the tests were unloaded. The load/deflection curves are nonlinear. However, if the sample was reloaded to the same load level, the load/deflection curve of the second loading case is very linear and its permanent set is much smaller. Similar behavior was observed in the SIR-C static test (as discussed in previous Section).

The second test is of a complete joint under cyclic load. The rivet pattern of the tested joint is shown in Figure 6. The total applied load is based on the design limit load (19,000 lbs for 22-rivets joint). The loading rate is 1 cycle per second. Results indicated that this joint failed at 2888 cycles, which is

very close to 4 times the design limit load cycles for the planned life of SIR-C mission (736 cycles from modal test, transportation, ferry flight and 3 missions). This design limit load cycle (Ref. 5) is considered to be very conservative.

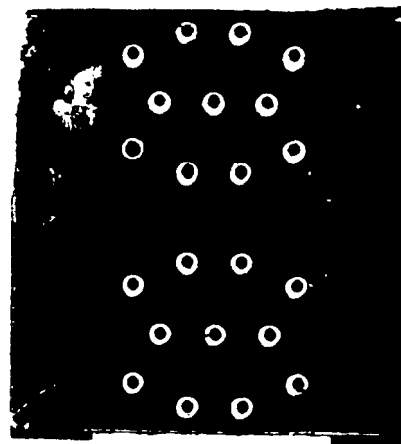


Fig. 6 Rivet Pattern of the Joint Subjected to Cyclic Test

SUMMARY

The strength validation of the SIR-C Antenna Core **Structure (ACS)** had been accomplished by loading selected members to more than 1.25 times flight limit loads (derived from conservative loads analysis by using the Modal **Mass** Acceleration Curve). No structural failures were observed from all loading configurations. Measured deformations were larger than those predictions, but these kinds of deformations were consistent with a multi-joint riveted structure and they were not detrimental. Testing results indicate that the measured axial forces of the test article agree very **well** (most critical **members** are within 10%) with the predictions from the finite element model. Better moment correlations have been achieved by modifying the end conditions of some members in the finite element **model**. In addition, the stiffness of members were also reduced, according to the testing **results** at 20% of the maximum applied loads, to account for the joint flexibility due to the rivet hole clearance and yielding. **All** these modifications were incorporated into the verification loads **model**. The strength of the joints was also verified by both